Multiplexed enrichment of rare DNA variants via sequence-selective and temperature-robust amplification

Lucia R. Wu[1], **Sherry X. Chen**[1], **Yalei Wu**[2], **Abhijit A. Patel**[3], and **David Yu Zhang**[iD,1,*]

[1]Department of Bioengineering, Rice University, Houston, TX 77030, USA

[2]Thermo Fisher, San Francisco, CA 94080, USA

[3]Department of Therapeutic Radiology, Yale School of Medicine, New Haven, CT 06510, USA

Abstract

Rare DNA-sequence variants hold important clinical and biological information, but existing detection techniques are expensive, complex, allele-specific, or don't allow for significant multiplexing. Here, we report a temperature-robust polymerase-chain-reaction method, which we term blocker displacement amplification (BDA), that selectively amplifies all sequence variants, including single-nucleotide variants (SNVs), within a roughly 20-nucleotide window by 1,000-fold over wild-type sequences. This allows for easy detection and quantitation of hundreds of potential variants originally at 0.1% in allele frequency. BDA is compatible with inexpensive thermocycler instrumentation and employs a rationally designed competitive hybridization reaction to achieve comparable enrichment performance across annealing temperatures ranging from 56 °C to 64 °C. To show the sequence generality of BDA, we demonstrate enrichment of 156 SNVs and the reliable detection of single-digit copies. We also show that the BDA detection of rare driver mutations in cell-free DNA samples extracted from the blood plasma of lung-cancer patients is highly consistent with deep sequencing using molecular lineage tags, with a receiver operator characteristic accuracy of 95%.

The economical and high-throughput detection and quantitation of nucleic acid sequence variants is a key goal on the road to widespread adoption of precision medicine, wherein optimal individualized treatment is provided to each patient based on their unique genetic and disease profile. Profiling rare nucleic acid variants with low allele frequencies, such as cancer mutations in cell-free DNA[1–4] or drug resistance in pathogen sub-populations[5–7],

---

presents a challenge for current molecular diagnostic technologies[8]. Allelespecific PCR methods[9–13] are difficult to scale to allow highly multiplexed rare variant detection, and deep sequencing approaches[14–16] are not economical because they waste a large majority of their read capacity on sequencing wild-type (WT) templates and amplicons. Sample enrichment to elevate the allele fractions of rare variants can allow economical sequencing-based rare variant profiling, but has been difficult to realize in highly multiplexed settings.

Past demonstrations of DNA-variant enrichment employ either selective depletion of WT sequences via hybridization[17–20] or selective PCR amplification of variants[21–24]. It has been challenging to scale these approaches to multiplexed enrichment of many different variants across different loci, because existing methods require that the operational reaction temperature sits in the 'Goldilocks' zone of every single blocker or probe. To elaborate, a WT sequence at a particular locus may bind to its probe or blocker to form a duplex with melting temperature T_M, and a variant at that locus would form a duplex with melting temperature $T_M- T_M$; only if the reaction temperature is in the range between these two values is there significant enrichment. Despite more than 40 years of biophysical studies, the melting temperature of a duplex sequence can only be predicted with a standard error of roughly 1.4 °C[25,26], corresponding to a 95% confidence interval that spans 5.6 °C. Empirical optimization is impractical in highly multiplexed systems, due to the combinatorially many interactions possible among DNA species that could each influence T_M.

Here, we present a simple method to enrich hundreds of potential DNA sequence variants from multiple genomic loci simultaneously. 'Simple' here denotes both that little to no empirical protocol optimization is needed, and that the DNA oligonucleotides employed are unmodified and broadly available. The key enabling innovation is a rationally designed competitive hybridization reaction that enables PCR not only to sensitively recognize and selectively amplify even SNVs at allele frequencies of 0.1%, but also to do so across a temperature window spanning 8 °C. Our variant allele enrichment method, blocker displacement amplification (BDA), significantly reduces both the cost and the complexity of profiling rare DNA variants, making genomics analysis more accessible and economical, both for researchers and for clinicians. Compared to other molecular diagnostic technologies used for detection and quantitation of rare alleles from clinical samples, BDA is unique in simultaneously providing good mutation sensitivity, high mutation multiplexing, fast turnaround, and low reagent and instrument cost (Table 1). Furthermore, in contrast to many proof-of-concept works in academic literature showing high mutation sensitivity against one or a few mutations, we here tested 156 single-nucleotide variants to show the sequence generality of BDA enrichment.

Blocker displacement amplification (BDA) design

BDA achieves enrichment through enforcing a differential hybridization yield of the forward primer P to a WT template versus a variant template, resulting in a difference in per-cycle amplification efficiency (Fig. 1). This differential amplification yield is compounded through multiple cycles of PCR to generate high enrichment factors.

Hybridization affinity difference is implemented using a blocker oligonucleotide B whose binding site on the template overlaps with the binding site of primer P. The simultaneous binding of P and B to the same template molecule is energetically unfavourable; thus, P and B compete in binding through a process of strand displacement[27].

The standard free energy of P displacing B is designed to be marginally positive (thermodynamically unfavourable) in the case of a WT template ($\Delta G°_{WT}$), but will be negative for a variant template due to the mismatch bubble or bulge formed between B and the variant template.

The values of $\Delta G°_{WT}$ and $\Delta G°_{Var}$ for a given set of sequences are only weakly dependent on the temperature of the PCR anneal step, because temperature affects the hybridization stability of both P and B to the template similarly. The competitive hybridization reaction pitting P versus B operates based on a similar principle as the toehold probe[27,28], which was shown both theoretically and experimentally to exhibit a large affinity difference between SNVs across a large range of temperatures and salinities at equilibrium. However, rapidly changing temperatures and the enzymatic extension of primers in a PCR reaction prevents the solution from attaining equilibrium, necessitating the development of a different, kinetics-driven model for simulating and analysing BDA behaviour. Our model provides design guidelines for maximizing enrichment performance, such as the stoichiometry of B and P. Details of our model are described in Supplementary Section 2.

For BDA to act as an enrichment assay, the sequences of the amplicon must faithfully correspond to the sequences of variant templates originally existing in solution. Consequently, P must bind a conserved sequence upstream of the loci with potential sequence variations (because amplicons always bear the sequence of the primer, and any variations in the primer-binding region of the template would be overwritten). The enrichment region of a BDA system thus corresponds to the nucleotides to which the blocker uniquely binds; templates with sequence variations within the enrichment region are preferentially amplified. The exact length of this enrichment region depends on the sequence in this region, but for the experiments shown here, this length ranges between 12 and 30 nucleotides (nt).

Any of a number of 3′ modifications could be used to effectively prevent the blocker from being extended by the DNA polymerase during PCR; examples include a minor groove binder[13], an inverted DNA nucleotide, and a 3-carbon spacer[29]. In this study, however, we opted for a simpler approach by adding 4 unmodified nucleotides at the 3′ end of the blocker that do not pair with the template. For DNA polymerases lacking 3′ to 5′ exonuclease activity, this 3′ 'terminator' sequence effectively blocks amplification for all sequences that we tested. We opted for this approach because such unmodified oligonucleotides are significantly less expensive than functionalized counterparts, and because the thermodynamics of their hybridization are better understood. Although only 2 nt of terminator sequence are needed to suppress blocker extension, we chose to use 4 nt terminator sequences to account for the possibility of potential variant templates that happen to match one of the terminator sequence nucleotides, and to account for possible oligonucleotide synthesis errors.

We performed detailed thermodynamics and kinetics modelling of the BDA reaction, in order to guide primer and blocker sequence design, as well as determine reaction conditions such as blocker to primer stoichiometry (Supplementary Section 2). The model consists of: (1) a mass-action kinetic simulation of the hybridization and enzyme elongation reactions at each anneal/extend step to calculate the per-step amplification yield for the WT and variant templates; and (2) a discrete simulation of each PCR cycle using the amplification yields from the previous step. Deviations between model and experimental results probably reflect both the simplicity of the model and the inaccuracy of literature-reported thermodynamics parameters[25,30].

Results

Non-pathogenic SNP results on genomic DNA

To quantitate the fold-enrichment of BDA on a representative set of SNVs, we first performed enrichment of non-pathogenic SNPs from human genomic DNA (gDNA).

NA18537 and NA18562 are gDNA samples extracted from two cell lines as part of the 1000 Genomes Project[31], and have well-characterized genotype information for many non-pathogenic SNPs. We generated gDNA samples with a variety of variant allele fractions (VAFs) by mixing the NA18537 and NA18562 samples at different ratios.

Figure 2a–c shows the design and performance of a BDA design for detecting the rs3789806 C > G SNP. The mean cycle threshold (Ct) values of the 0.01% VAF and the 0% VAF samples are 7.4 standard deviations apart, indicating much greater than 99% statistical confidence in a difference of true values. The results further imply that more than 10,000× SNV enrichment is achieved. The regression line between the Ct and the VAF has a slope of 3.45, indicating that PCR amplification of the variant template occurs at near 100% efficiency.

BDA is a sequence-general method that effectively enriches all SNVs regardless of the nucleotide identities of the variant and WT. Figure 2d summarizes the quantitative PCR (qPCR) results for 24 separate BDA systems, representing two instances of each of the 12 possible SNV/WT nucleotide pairs; for a large majority of WT/SNV pairs, the median enrichment observed was greater than 1,000. The results in Fig. 2d are for preliminary BDA designs that were not subjected to empirical optimization; our later experiments (Supplementary Section 4) suggest that some primer/blocker sequence adjustments may lead to even better enrichment performance.

Some variability observed in the Ct of the 0% VAF sample is believed to be primarily due to the stochastic nature of the early cycles of PCR, specifically in (1) enzyme misincorporation errors and (2) WT amplification yields. These hypotheses are supported by the observation that larger gDNA input quantities result in smaller variability in 0% VAF Ct values; at 4 ng and 200 ng gDNA input, the standard deviation of 96 BDA reactions with 0% VAF were observed to be 4.02 and 0.48 cycles, respectively (Supplementary Section 5).

Temperature robustness

An important and distinguishing feature of BDA is the broad temperature range over which it effectively enriches variants. Figure 3a shows the enrichment performance of the BDA system across anneal/extend step temperatures ranging between 55 and 65 °C. The Ct values for 1% and 0% VAF samples maintain a difference of more than 10 cycles for anneal/extend temperatures of 56–64 °C. Below 56 °C, DNA polymerase activity decreases, resulting in poor amplification; above 64 °C, the hybridization of the primer to either template becomes unstable, also resulting in poor amplification. BDA temperature robustness is sequence-generic; Fig. 3c shows the observed Ct values for 6 WT/variant pairs at 100%, 1% and 0% VAF. The Ct values of triplicate reactions are generally consistent across all temperatures tested.

As a contrast to the temperature robustness of BDA, we also tested enrichment PCR on the rs3789806 SNP using locked nucleic acid (LNA) clamp oligonucleotides at a variety of temperatures (Fig. 3b; see also Supplementary Section 6). The LNA clamp provided high amplification yield and significant discrimination between 1% and 0% VAF only at anneal/extend temperatures of 56–57 °C. Our expectation is that similar temperature sensitivities would be observed for other existing PCR enrichment methods[21,24]. We also attempted to test PCR enrichment using a PNA clamp, but had trouble dissolving the PNA oligonucleotide into the PCR buffer, and consequently did not observe significant Ct for SNVs.

Multiplex BDA

The broad temperature robustness of BDA manifests as a strong advantage in the design and operation of multiplexed allele enrichment systems. To allow multiplexed readout in qPCR, we designed different Taqman probes to each of three different target genes of interest (Fig. 4a); the Taqman probes bind a sequence downstream of the mutation of interest, and thus are not allele-specific. Each Taqman probe bears a different fluorophore, allowing us to simultaneously detect and quantitate all three BDA systems. Figure 4b shows the qPCR results for 3-plex BDA on cancer mutations using 3 different Horizon Discovery cell-free DNA (cfDNA) reference samples. The lowest VAF sample (left-most dotted box in Fig. 4b) corresponds to 0.1% EGFR-T790M and EGFR-L858R, and 0.13% NRAS-Q61K, corresponding to roughly 9 molecules of each of the former two and 12 molecules of the latter. The relatively larger error bars for this lowest VAF sample are likely to reflect Poisson variation in the number of variant molecules in each sample.

To demonstrate higher multiplexing capability, we next performed 9-plex BDA (Fig. 4c). Due to the limited number of independent colour channels available on conventional qPCR instruments (we used a Biorad CFX96), we used 9 different Taqman probes across 3 colours: thus, each colour denotes amplification of any of 3 potential gene targets. The Ct values observed are consistent with expectations based on single-plex results, and the decrease of primer and blocker concentrations necessary for allowing 9-plex amplification does not appear to significantly affect Ct values when cycle times are lengthened to compensate. Importantly, the multiplex enrichment experiments summarized in Fig. 4a–c represent our first-try designs, and did not undergo any empirical optimization. We believe that

significantly higher multiplexed allele enrichment can be achieved with BDA; however, methods of readout more sensitive and multiplexed than traditional qPCR instruments are needed to fully capture the value of multiplex BDA.

Finally, the temperature robustness of BDA also uniquely allows the use of portable and inexpensive thermocycling equipment to detect and enrich sequence variants. Fig. 4d shows the polyacrylamide gel electrophoresis results of using a 3-plex BDA system on the MiniPCR, an instrument with dimensions of roughly $5 \times 13 \times 10$ cm and a commercially available retail price of US\$650[32,33]. To the best of our knowledge, this is the first time that SNVs have been reliably distinguished in such portable and economical PCR instruments. BDA is also broadly compatible with many different commercial PCR instruments; we have experimentally validated BDA on five different platforms by Biorad, Applied Biosystems, Eppendorf, and Qiagen (data not shown).

Hotspot multiplexing

BDA enriches all variants with sequences differing from the WT in the enrichment region. Sanger sequencing results of amplicons from BDA enrichment of 0%, 0.1% and 1% VAF samples (Fig. 5a) verify that rare variants become the dominant amplicons after BDA, while amplicons of WT samples retain WT status. This means that for a typical 20 nt enrichment region, 60 SNVs can be simultaneously enriched by a single BDA system, albeit with differing fold-enrichment because of varying $G°$ values (see Supplementary Section 2). In this regard, BDA is significantly superior to allele-specific PCR approaches (such as amplification-refractory mutation system (ARMS)) — each plex of BDA is the equivalent of a 60-plex ARMS.

A clear fit for the large enrichment region of BDA is the enrichment of clustered cancer mutations, also known as hotspots. To demonstrate the suitability of BDA to hotspot mutation enrichment, we applied a single-plex BDA system to the codon 12/13 hotspot of the KRAS oncogene, responsible for resistance to cetuximab in colorectal cancer patients[34]. We diluted five reference cell-line gDNA samples bearing different KRAS mutations (Horizon Discovery) with WT cell-line DNA to generate 0.1% VAF samples. These samples were subsequently enriched by BDA, and the amplicons were Sanger sequenced; the results are shown in Fig. 5b. In all cases, the mutations were enriched significantly to produce clear Sanger sequencing peaks.

To rigorously demonstrate that BDA does enrich all potential variants in the enrichment region, we systematically designed 2 sets of synthetic DNA templates bearing SNVs, corresponding to all SNVs in a 18 nt enrichment region on chromosome 5 and a 21 nt enrichment region on chromosome 11 (Fig. 5c). The experimentally observed distribution of Ct values for these SNVs range between 7 and 14, with mean and median both at roughly 10.5 (corresponding to over 1,000-fold enrichment). Note that the same BDA primer/blocker system was used to enrich all 54 SNVs in the left panel, and another BDA system was used to enrich all 63 SNVs in the right panel.

BDA is an enrichment technology that can be combined with either qPCR or sequencing readout. Fig. 5b shows that BDA plus Sanger can identify the exact variant that was

enriched. In the context of qPCR, two separate BDA reactions should be run to determine the enriched variant's identity: one with a standard WT blocker, and one containing both the WT blocker and a blocker to the variant of interest. Significant amplification (low Ct) of a sample with the second BDA reaction indicates that the sample contains an incidental variant other than the variant of interest (Fig. 5d).

Improving BDA enrichment

The allele enrichment achieved by BDA is limited by two factors: (1) DNA polymerase nucleotide misincorporation events that create de novo variants subsequently enriched by BDA[35], and (2) imperfect suppression of WT template amplification by the blocker. Limitation (1) can be mitigated through the use of high-fidelity DNA polymerases with 3′ to 5′ proofreading activity, and (2) can be mitigated through the use of a second blocker for the reverse primer (Supplementary Section 10). For different Variant/WT pairs, either (1) or (2) may be dominant; thus, addressing each of these two problems results in improved BDA performance for a subset of Variant/WT sequence pairs. Judicious application of these two approaches allows BDA enrichment to be enhanced for a large fraction of, if not all, Variant/WT pairs.

BDA qPCR quantitation

BDA in conjunction with qPCR can be used to quantitate the absolute number of both variant and WT molecules; Fig. 6a shows one implementation. Here, the DNA sample is split asymmetrically with 10% amplified using BDA primers without the blocker, and the other 90% is amplified using the standard BDA primer/blocker combination. Using control samples as calibration, we can determine both the Ct delay of variant templates and the efficiency of qPCR. These two pieces of information, in conjunction with the observed Ct values for the two sub-samples, allows us to determine both the total number of molecules of either variant or WT, and the VAF. From here, simple arithmetic produces estimates for the number of variant and WT molecules in the original sample. Where the number of original variant molecules is estimated to be less than 0.5, we assume that the true number of variant molecules is zero. See Supplementary Section 11 for mathematical details on BDA quantitation. For comparison, we also performed quantitation using Biorad droplet digital PCR (ddPCR), typically considered the gold standard for DNA quantitation today.

We tested BDA and ddPCR quantitation on two types of samples: mixtures of cell-line gDNA, and Horizon Discovery reference cfDNA. The former samples were tested for non-pathogenic SNPs, and the latter samples were tested on cancer driver mutations. The total amount and the VAF were determined via computer-generated quasi-random numbers; Horizon cfDNA samples were diluted with cell-line gDNA to construct samples with lower VAFs. In both sample types, BDA and ddPCR quantitation showed similar performance (Fig. 5b and Supplementary Section 11). Based on these results, we felt that BDA quantitation accuracy is comparable to that of ddPCR, and likely to be accurate to within 50% of true values. ddPCR showed slightly higher consistency/precision, but also displayed a consistent bias from the true values to lower numbers of both variant and WT molecules by about a factor of two. We believe this may be due to losses in ddPCR droplet generation and reading (for example, imperfect droplets that cannot be read, or leftover samples that were

not dropletized). Note that ddPCR is incapable of detecting more than one mutation within a DNA sample (at least, as currently commercially implemented), whereas BDA is capable of simultaneously enriching tens to hundreds of potential variants.

Clinical cell-free DNA analysis

Cell-free DNA consists of short (approx. 160 nt) double-stranded DNA molecules present in blood plasma at low concentrations of roughly 5 to 20 ng ml^{-1} (refs [1,2]). Cancer-specific mutations in cfDNA can be used for noninvasive therapy guidance or recurrence monitoring[3,4,36] and even holds potential as cancer early detection biomarkers[37], but are present at low VAFs of below 1%. The combination of low total amount and low VAF renders cfDNA challenging to analyse for mutations using conventional PCR and next-generation sequencing (NGS) methods.

We used BDA to analyse the cfDNA from the blood plasma of 24 lung cancer patients, collected between January 2013 and November 2014 (see also Supplementary Section 12); informed consent was obtained from all subjects. As a comparison, the cfDNA mutations were also profiled by deep sequencing using molecular lineage tags to suppress sequencing and PCR errors via a previously published method[35] (Fig. 6c). The inferred number of mutant molecules are summarized in Fig. 6d, and the concordance between the two methods is summarized with the receiver operator characterizeristic (ROC) curve. Both methods called positives for 17 samples and negatives for 7 samples, but were discordant for 2 samples: BDA quantitated 1 mutant molecule for a sample that DeepSeq quantitated 0, and BDA quantitated 0 mutant molecules for a sample that DeepSeq quantitated 3. In both cases, unequal distribution of mutant cfDNA molecules during sample splitting given that a low discrete number of mutant molecules is likely.

The VAFs quantitated by BDA and deep sequencing are comparatively plotted in Fig. 6e; there is a moderately strong correlation constant of $r^2 = 0.72$. As mentioned previously, Poisson limitations of sample splitting for low numbers of mutant molecules probably contributes to the discrepancy. Additionally, it has been observed that tumour-derived cfDNA fragments have somewhat different length distribution profiles than healthy cfDNA[38,39], so the choice of amplicon length may impact the observed VAF. While our BDA quantitation experiments on reference samples (Fig. 6b) show some inaccuracy, it is also well known that NGS exhibits sequence bias that limits quantitation accuracy[40–42]. Consequently, at this point, we do not have strong evidence to preferentially trust either BDA or deep sequencing over the other. However, insofar as the two independent methods generally agree on the majority of clinical samples, our results provide positive validation for both technologies.

Discussion

BDA overcomes the temperature sensitivity that limit all existing PCR enrichment methods through a rationally designed competitive hybridization reaction. This temperature robustness translates into practical advantages for molecular diagnostics and genomics research in at least two ways: facilitating the highly multiplexed enrichment of many SNVs, and enabling the use of more portable and economical PCR instruments with lower

temperature accuracy and uniformity. BDA does not rely on expensive functionalized DNA oligonucleotides, is broadly compatible with many enzymes, and is tolerant to instrument temperature inaccuracies and non-uniformity; consequently, BDA is highly economical and accessible to both clinicians and researchers. Systematic experimental validation of BDA enrichment on 156 different SNVs, and on a variety of samples ranging from synthetic templates to cell-line gDNA to clinical blood samples, shows the robustness of BDA as a rare variant enrichment and detection method.

An immediate area of clinical application for BDA technology is noninvasive cancer recurrence monitoring based on cfDNA. NGS-based solutions for analysing cfDNA are too costly to be repeatedly and regularly applied, while low-multiplex PCR methods are insufficient for high clinical sensitivity. In this study, we demonstrated multiplex BDA targeting 9 different genomic regions within the same reaction; simultaneously, we showed that each BDA system is capable of enriching and detection more than 50 variants. Together, these indicate that roughly 500 different SNVs can be detected at roughly 0.1% allelic frequency in a single low-cost and rapid reaction. Additional development and optimization of the BDA technique could potentially further extend the number of mutations detected and enriched to over 1,000 — which suggests that rare variant discovery could be another potential application for BDA.

In addition to cancer diagnostic applications in a reference laboratory setting, BDA may also facilitate point of care or field-use nucleic acid testing for other applications in which rare variants exhibit disproportionate impact, such as antibiotic-resistant subpopulations of infectious diseases. Alternatively, BDA could enable much more economical discovery and profiling of rare alleles at a population level, wherein DNA samples from thousands of different individuals are combined to search for rare germline differences[43]; applications for population genetics include human genome-wide association studies (GWAS)[44] and agricultural seed selection.

The fold-enrichment achieved for SNVs using the basic BDA implementation (lacking a high-fidelity enzyme and dual blocking) was observed to be between approximately 300 and 30,000, varying based on SNV and WT sequences. This performance could be improved through empirical optimization, as the DNA hybridization thermodynamics parameters we used for designing BDA systems are known to be imperfect[25]. In settings where open-tube procedures are allowed (such as NGS library preparation), multiple rounds of BDA enrichment followed by dilution could result in theoretically unlimited rare mutation sensitivity.

Methods

Oligonucleotides and repository samples

Primers, non-modified blockers, C3 spacer-modified blockers, and synthetic DNA template oligonucleotides were purchased from Integrated DNA Technologies. LNA clamp oligonucleotides were purchased from Exiqon. Primers and blockers were purchased as standard desalted DNA oligonucleotides, and synthetic templates as standard desalted ultramers; they were resuspended in 1× TE buffer (purchased as 100× stock from Sigma

Aldrich). Solutions of DNA oligonucleotides were stored at 4 °C, and LNA at −20 °C. Human cell-line gDNA repository samples (NA18562 and NA18537) were purchased from Coriell Biorepository, and stored at −20 °C. The two gDNA samples were mixed at various ratios to create samples containing different proportions of a specific allele. Cancer mutation reference gDNA and cfDNA samples(Multiplex I cfDNA Reference Standard Set and Structural Multiplex cfDNA Reference Standard) were purchased from Horizon Discovery, and stored at 4 °C. Dilution of gDNA samples and synthetic DNA templates were made in 1× TE buffer with 0.1% TWEEN 20 (Sigma Aldrich).

Taq polymerase qPCR protocol

BDA qPCR assays were performed on a CFX96 Touch Real-Time PCR Detection System using 96-well plates (Bio-Rad). In a typical Taq polymerase-based assay, PowerUp SYBR Green Master Mix (Thermo Fisher) was used for enzymatic amplification and fluorescence signal generation; primer concentrations were 400 nM each, and blocker concentration was 4 μM, unless otherwise stated. Per-well gDNA sample input ranged between 4 ng and 400 ng per well; reactions were performed in triplicates, and the total volume was 10 μl in each well. Thermal cycling started with a 3 min incubation step at 95 °C for polymerase activation, followed by 66 repeated cycles of 10 s at 95 °C for DNA denaturing and 30 s at 60 °C for annealing/extension (abbreviated as 95 °C:3min–(95 °C:10s–60 °C:30s) × 66), unless otherwise stated. Temperature robustness assays (Fig. 3a–d) used different annealing/extension temperatures ranging between 55 and 65 °C, but with the same step time of 30 s. Blocker stoichiometry assays (Fig. 4c) used different blocker concentrations ranging between 400 nM and 20 μM.

Ct determination

Raw qPCR traces were processed using custom Matlab functions and scripts. The background fluorescence signal was calculated as the average of the raw fluorescence of the first 10–15 cycles, and was subtracted from all cycle fluorescence values before calculating cycle threshold Ct. With the exception of the 9-plex BDA experiment (Fig. 3e), Ct values are calculated as the interpolated fractional cycles at which 20% of the final fluorescence (average of the last 4 data points) is achieved; the Ct value is recorded as >max cycles if the final fluorescence was lower than 200 relative fluorescence units (RFU).

Sanger sequencing

PCR reactions were performed as described in 'Taq polymerase qPCR protocol' and 'KAPA HiFi Polymerase Protocol', with the number of PCR cycles set to 45. The intercalating dye SYTO 13 was not included in KAPA HiFi experiments in which amplicons were Sanger sequenced. PCR products were purified and sequenced by Genewiz Custom Sanger Sequencing services.

Multiplex BDA assays of non-pathogenic mutations

9 BDA Taqman assays were performed simultaneously in each well; primer concentrations were 50 nM each, blockers were 500 nM each, and Taqman probes were 50 nM each; 4 ng gDNA input was added to each well, and the reaction volume was 10 μl. PowerUp SYBR

Green Master Mix was used; experiments were performed on the Bio-Rad CFX96 instrument using a 95 °C:3 min–(95 °C:10 s–60 °C:4 min) × 50 thermal cycling protocol. For Ct determination, the threshold was 10% of the final fluorescence.

Multiplex BDA assays on miniPCR

The 3 BDA amplification systems were used to simultaneously amplify 3 SNP alleles at distinct genomic regions. The amplicons for each BDA system were different by roughly 30 nt to allow bands to be easily distinguished during polyacrylamide gel electrophoresis.

Primer concentrations were 100 nM each, blockers were 1 μM each; 4 ng gDNA input (NA18537) was added to each well, and the reaction volume was 25 μl. PowerUp SYBR Green Master Mix was used; experiments were performed on the MiniPCR instrument using a 95 °C:3 min–(95 °C:10 s–60 °C:2 min) × 30 thermal cycling protocol. The PCR product was then analysed by precast 10% TBE-Urea gel (Invitrogen), which was stained with SYBR Safe dye (Thermo Fisher) after electrophoresis; a 50 bp DNA ladder (New England Biolabs) was used for reference.

Multiplexed BDA assays of cancer mutations in horizon cfDNA samples

Three BDA systems were used to simultaneously amplify 3 cancer mutations; primer concentrations were 100 nM each, blockers were 1 μM each, and Taqman probes were 100 nM each; 30 ng Horizon cfDNA input was added to each well, and the reaction volume was 10 μl. PowerUp SYBR Green Master Mix was used; experiments were performed on the Bio-Rad CFX96 instrument using a 95 °C:3 min–(95 °C:10 s–60 °C:2 min) × 66 thermal cycling protocol.

Systematic hotspot analysis

Each of the synthetic templates used for the systematic hotspot analysis experiments in Fig. 5c were ordered as gBlocks from IDT. After dilution, synthetic template concentrations were quantitated by qPCR using the primers without blocker; the concentrations of the forward and reverse primers were 400 nM each, and the concentration of the synthetic template was approximately 20 fM. The Ct values of the synthetic templates were compared to the Ct value of 200 ng per well gDNA assayed with the same primers, and the concentrations of the synthetic templates were normalized based on the Ct difference (see Supplementary Section 9 for details).

Each synthetic template amplified with BDA using 400 nM of each primer and 4 μM of blocker; the synthetic template concentration was equivalent to the target concentration in 2.5 ng μl^{-1} gDNA. The Ct was calculated as the Ct difference between the synthetic template and 2.5 ng μl^{-1} (25 ng per well) gDNA, which was assayed with the same BDA set. The qPCR protocol was the same as in 'Taq polymerase qPCR protocol', and the WT gDNA sample was NA18562.

KRAS mutation disambiguation via qPCR

Oligo concentrations and qPCR protocol were the same as in 'Taq polymerase qPCR protocol'; the second blocker (that is, mutant-specific blocker) was also added to achieve a

final concentration of 4 μM; gDNA was 4 ng per well. The WT sample was NA18562, and was mixed with Horizon KRAS mutation reference samples to achieve 10% mutation VAF.

KAPA HiFi polymerase protocol

Oligo concentrations were the same as in 'Taq polymerase qPCR protocol'; we used a KAPA HiFi Hotstart PCR Kit (Kapa Biosystems) following the instructions. 10 μM SYTO 13 dye (Thermo Fisher) was added to the reactions to enable fluorescence signal generation.

Dual BDA protocol

Primer concentrations and qPCR protocol were the same as in 'Taq polymerase qPCR protocol'; both forward and reverse blockers had final concentrations of 4 μM each; gDNA sample input amount was 400 ng per well.

BDA quantitation protocol

Each cfDNA or gDNA sample was asymmetrically split into a 90% portion for mutant allele quantitation, and a 10% portion for calibration of total concentration.

90% of the sample was mixed with primers and the WT blocker, and 10% of the sample was mixed with primers only. qPCR reactions were performed using the same oligonucleotide concentrations, qPCR mastermix, and thermal cycling protocol as described in 'Taq polymerase qPCR protocol'.

ddPCR quantitation protocol

ddPCR assays were performed on a QX200 Droplet Digital PCR System (Bio-Rad). The primers, WT and variant Taqman probes, DNA sample, and ddPCR Supermix for Probes (Bio-Rad) were mixed and loaded onto the DG8 cartridges (Bio-Rad), and the droplets were generated using the QX200 Droplet Generator (Bio-Rad) and Droplet Generation Oil for Probes (Bio-Rad). Primer concentrations were 1 μM each, and Taqman probe concentrations were 500 nM each. Per well gDNA sample input was below 60 ng; the total volume was 20 μl in each well. Thermal cycling started with a 10 min incubation step at 95 °C for polymerase activation, followed by 40 repeated cycles of 30 s at 94 °C for DNA denaturing and 1 min at 60 °C for annealing/extension; an enzyme deactivation step of 10 min at 98 °C was added at the end, and the samples were held at 4 °C before the next step (abbreviated as 95 °C:10 min– (94 °C:30 s–60 °C:1 min) × 40–98 °C:10 min–4 °C:hold). After PCR, the plate was loaded onto the QX200 Droplet Reader (Bio-Rad), and the droplet fluorescence data was generated. We performed analysis on the droplet fluorescence data using a custom Matlab code.

Validation of BDA quantitation

We prepared 5 gDNA samples and 4 cfDNA samples with randomly generated values of VAF and total concentration. The gDNA samples were made by mixing NA18562 (as WT) and NA18537 (as variant), and the cfDNA samples were made by mixing the 5%, 1%, 0.1% variant, and 100% WT samples in the Horizon Multiplex I cfDNA Reference Standard Set. Each sample was split into a 50% portion for BDA quantitation and a 50% portion for ddPCR quantitation. Experiments were performed in duplicates.

Blood sample collection, cfDNA extraction and VAF quantitation

Plasma samples were obtained from patients who had provided informed consent under a study protocol that was approved by the Human Investigation Committee at Yale University (protocol number 0909005749). We used QIAamp MinElute Virus Vacuum Kit (Qiagen) and QIAamp MinElute Virus Spin Kit (Qiagen) for purifying DNA from 1 ml plasma following the handbook protocols. The elution volume for each sample was 25 μl in AVE buffer (Qiagen). Samples 1–9 were extracted using the QIAamp MinElute Virus Vacuum Kit; after extraction, each sample was split into a 50% portion for deep sequencing and a 50% portion for BDA. Samples 10–19 were split as plasma; 50% (1 ml) of each sample were extracted with the QIAamp MinElute Virus Vacuum Kit followed by deep sequencing, and the other 50% (1 ml) was extracted with the QIAamp MinElute Virus Spin Kit followed by BDA quantitation. Experiments were not replicated, due to limited clinical sample volume.

Data availability

The reference and sample-specific gDNA sequence data are available from the NCBI Nucleotide database (https://www.ncbi.nlm.nih.gov/nuccore/) and the 1000 Genomes Project website (http://www.internationalgenome.org/). The version of the human genome assembly used is GRCh37.p13 (GenBank assembly accession number GCA_000001405.14). All other data supporting the findings of this study are available within the paper and its Supplementary Information files.

Code availability

The Matlab codes used for BDA simulation and ddPCR data processing are available in the Supplementary Information.

Supplementary Material

Refer to Web version on PubMed Central for supplementary material.

Acknowledgments

References

1. Bettegowda C, et al. Detection of circulating tumor DNA in early- and late-stage human malignancies. Sci. Transl. Med. 2014; 6:224ra24.

2. Wan JCM, et al. Liquid biopsies come of age: towards implementation of circulating tumour DNA. Nat. Rev. Cancer. 2017; 17:223–238. [PubMed: 28233803]

3. Heitzer E, Ulz P, Geigl JB. Circulating tumor DNA as a liquid biopsy for cancer. Clin. Chem. 2015; 61:112–123. [PubMed: 25388429]

4. Schwarzenbach H, Hoon DSB, Pantel K. Cell-free nucleic acids as biomarkers in cancer patients. Nat. Rev. Cancer. 2011; 11:426–437. [PubMed: 21562580]

5. Lewis K. Persister cells, dormancy and infectious disease. Nat. Rev. Microbiol. 2007; 5:48–56. [PubMed: 17143318]

6. Jones SE, Lennon JT. Dormancy contributes to the maintenance of microbial diversity. Proc. Natl Acad. Sci. USA. 2010; 107:5881–5886. [PubMed: 20231463]

7. Ford CB, et al. *Mycobacterium tuberculosis* mutation rate estimates from different lineages predict substantial differences in the emergence of drug-resistant tuberculosis. Nat. Genet. 2013; 45:784– 790. [PubMed: 23749189]

8. Khodakov D, Wang C, Zhang DY. Diagnostics based on nucleic acid sequence variant profiling: PCR, hybridization, and NGS approaches. Adv. Drug Deliv. Rev. 2016; 105:3–19. [PubMed: 27089811]

9. Newton CR, et al. Analysis of any point mutation in DNA. The amplification refractory mutation system (ARMS). Nucleic Acids Res. 1989; 17:2503–2516. [PubMed: 2785681]

10. Vargas DY, Kramer FR, Tyagi S, Marras SA. Multiplex real-time PCR assays that measure the abundance of extremely rare mutations associated with cancer. PLoS ONE. 2016; 11:e0156546. [PubMed: 27244445]

11. Gonzalez de Castro D, et al. A comparison of three methods for detecting KRAS mutations in formalin-fixed colorectal cancer specimens. Br. J. Cancer. 2012; 107:345–351. [PubMed: 22713664]

12. Morlan J, Baker J, Sinicropi D. Mutation detection by real-time PCR: a simple, robust and highly selective method. PLoS ONE. 2009; 4:e4584. [PubMed: 19240792]

13. Didelot A, et al. Competitive allele specific TaqMan PCR for KRAS, BRAF and EGFR mutation detection in clinical formalin fixed paraffin embedded samples. Exp. Mol. Pathol. 2012; 92:275– 280. [PubMed: 22426079]

14. Lanman RB, et al. Analytical and clinical validation of a digital sequencing panel for quantitative, highly accurate evaluation of cell-free circulating tumor DNA. PLoS ONE. 2015; 10:e0140712. [PubMed: 26474073]

15. Kinde I, Wu J, Papadopoulos N, Kinzler KW, Vogelstein B. Detection and quantification of rare mutations with massively parallel sequencing. Proc. Natl Acad. Sci. USA. 2011; 108:9530–9535. [PubMed: 21586637]

16. Newman AM, et al. An ultrasensitive method for quantitating circulating tumor DNA with broad patient coverage. Nat. Med. 2014; 20:548–554. [PubMed: 24705333]

17. Pel J, et al. Nonlinear electrophoretic response yields a unique parameter for separation of biomolecules. Proc. Natl Acad. Sci. USA. 2009; 106:14796–14801. [PubMed: 19706437]

18. Kidess E, et al. Mutation profiling of tumor DNA from plasma and tumor tissue of colorectal cancer patients with a novel, high-sensitivity multiplexed mutation detection platform. Oncotarget. 2015; 6:2549. [PubMed: 25575824]

19. Wang JS, Zhang DY. Simulation-guided DNA probe design for consistently ultraspecific hybridization. Nat. Chem. 2015; 7:545–553. [PubMed: 26100802]

20. Song C, et al. Elimination of unaltered DNA in mixed clinical samples via nuclease-assisted minor-allele enrichment. Nucleic Acids Res. 2016; 44:e146. [PubMed: 27431322]

21. Orum H, et al. Single base pair mutation analysis by PNA directed PCR clamping. Nucleic Acids Res. 1993; 21:5332–5336. [PubMed: 8265345]

22. Arcila M, Lau C, Nafa K, Ladanyi M. Detection of KRAS and BRAF mutations in colorectal carcinoma: roles for high-sensitivity locked nucleic acid-PCR sequencing and broad-spectrum mass spectrometry genotyping. J. Mol. Diagnost. 2011; 13:64–73.

23. Li J, et al. Replacing PCR with COLD-PCR enriches variant DNA sequences and redefines the sensitivity of genetic testing. Nat. Med. 2008; 14:579–584. [PubMed: 18408729]

24. Milbury CA, Li J, Makrigiorgos GM. Ice-COLD-PCR enables rapid amplification and robust enrichment for low-abundance unknown DNA mutations. Nucleic Acids Res. 2011; 39:e2. [PubMed: 20937629]

25. SantaLucia J Jr, Hicks D. The thermodynamics of DNA structural motifs. Annu. Rev. Biophys. Biomol. Struct. 2004; 33:415–440. [PubMed: 15139820]

26. Owczarzy R, Moreira BG, You Y, Behlke MA, Walder JA. Predicting stability of DNA duplexes in solutions containing magnesium and monovalent cations. Biochemistry. 2008; 47:5336–5353. [PubMed: 18422348]

27. Zhang DY, Chen SX, Yin P. Thermodynamic optimization of nucleic acid hybridization specificity. Nat. Chem. 2012; 4:208–214. [PubMed: 22354435]

28. Wu LR, et al. Continuously tunable nucleic acid hybridization probes. Nat. Methods. 2015; 12:1191–1196. [PubMed: 26480474]

29. Dobosy JR, et al. RNase H-dependent PCR (rhPCR): improved specificity and single nucleotide polymorphism detection using blocked cleavable primers. BMC Biotechnol. 2011; 11:80. [PubMed: 21831278]

30. Wang C, Bae JH, Zhang DY. Native characterization of nucleic acid motif thermodynamics via non-covalent catalysis. Nat. Commun. 2016; 7:10319. [PubMed: 26782977]

31. 1000 Genomes Project Consortium. An integrated map of genetic variation from 1,092 human genomes. Nature. 2012; 491:56–65. [PubMed: 23128226]

32. Marx V. PCR heads into the field. Nat. Methods. 2015; 12:393–397. [PubMed: 25924072]

33. http://www.minipcr.com/

34. Lievre A, et al. KRAS mutation status is predictive of response to cetuximab therapy in colorectal cancer. Cancer Res. 2006; 66:3992–3995. [PubMed: 16618717]

35. Narayan A, et al. Ultrasensitive measurement of hotspot mutations in tumor DNA in blood using error-suppressed multiplexed deep sequencing. Cancer Res. 2012; 72:3492–3498. [PubMed: 22581825]

36. Garcia-Murillas I, et al. Mutation tracking in circulating tumor DNA predicts relapse in early breast cancer. Sci. Transl. Med. 2015; 7:302ra133.

37. Imperiale TF, et al. Multitarget stool DNA testing for colorectal-cancer screening. N. Engl. J. Med. 2014; 370:1287–1297. [PubMed: 24645800]

38. Underhill HR, et al. Fragment length of circulating tumor DNA. PLoS Genet. 2016; 12:e1006162. [PubMed: 27428049]

39. Mouliere F, et al. High fragmentation characterizes tumour-derived circulating DNA. PLoS ONE. 2011; 6:e23418. [PubMed: 21909401]

40. Aird D, et al. Analyzing and minimizing PCR amplification bias in Illumina sequencing libraries. Genome Biol. 2011; 12:R18. [PubMed: 21338519]

41. Ross MG, et al. Characterizing and measuring bias in sequence data. Genome Biol. 2013; 14:R51. [PubMed: 23718773]

42. Laehnemann D, Borkhardt A, McHardy AC. Denoising DNA deep sequencing data: high-throughput sequencing errors and their correction. Brief. Bioinform. 2016; 17:154–179. [PubMed: 26026159]

43. Forbes SA, et al. COSMIC: mining complete cancer genomes in the Catalogue of Somatic Mutations in Cancer. Nucleic Acids Res. 2010; 39:D945–D950. [PubMed: 20952405]

44. Welter D, et al. The NHGRI GWAS Catalog, a curated resource of SNP-trait associations. Nucleic Acids Res. 2014; 42:D1001–D1006. [PubMed: 24316577]

45. Hardenbol P, et al. Multiplexed genotyping with sequence-tagged molecular inversion probes. Nat. Biotechnol. 2003; 21:673–678. [PubMed: 12730666]

46. Hiatt JB, Pritchard CC, Salipante SJ, O'Roak BJ, Shendure J. Single molecule molecular inversion probes for targeted, high-accuracy detection of low-frequency variation. Genome Res. 2013; 23:843–854. [PubMed: 23382536]

47. Narayan A, Bommakanti A, Patel AA. High-throughput RNA profiling via up-front sample parallelization. Nat. Methods. 2015; 12:343–346. [PubMed: 25730493]
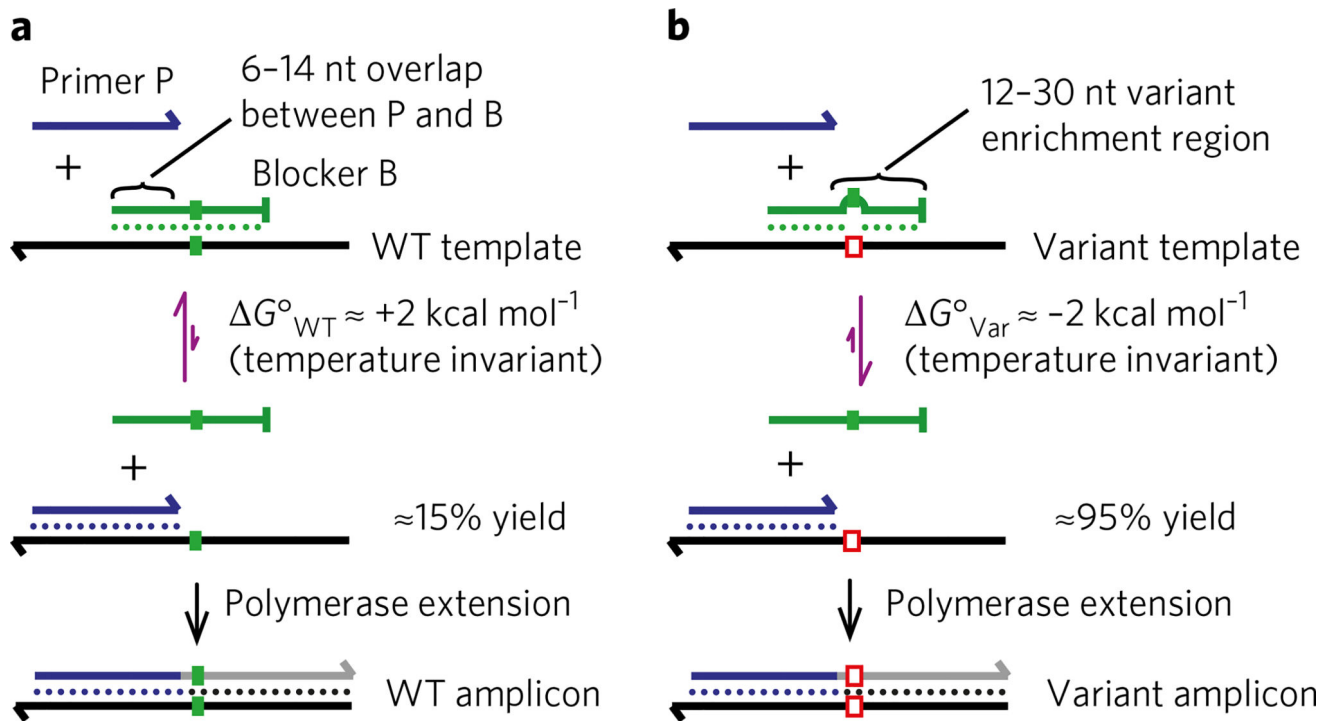
Fig. 1. Temperature-robust enrichment of rare alleles by blocker displacement amplification (BDA)

a, The blocker (green) is designed to be perfectly complementary to a known WT template sequence. The 3′ end of the forward primer sequence (blue) is identical to the 5′ end of the blocker sequence; this 6–14 nt overlap region induces molecular competition between the primer and blocker, so that primer and blocker hybridization to the same template molecule is mutually exclusive. See Supplementary Section 1 for primer and blocker sequence design considerations. **b**, The 3′ end of the blocker contains a 12–30 nt sequence that is not present in the primer. Any sequence variation in the template in this region will manifest a mismatch bubble or bulge in the blocker–template duplex, increasing the favourability of the primer to displace the blocker. A single-nucleotide variation with a characteristic $\Delta G°$ of 4 kcal mol^{-1} (ref. [27]) would cause the $\Delta G°$ of the primer displacing the blocker on the variant template to drop from + 2 kcal mol^{-1} to –2 kcal mol^{-1}, resulting in approximately 95% hybridization yield at equilibrium. The difference in the primer displacement favourability results in a difference in per-cycle amplification yield. The amplicon generated by a round of PCR amplification bears the allele of the template, so the amplification yield difference is compounded across many PCR cycles to over 1,000-fold enrichment.
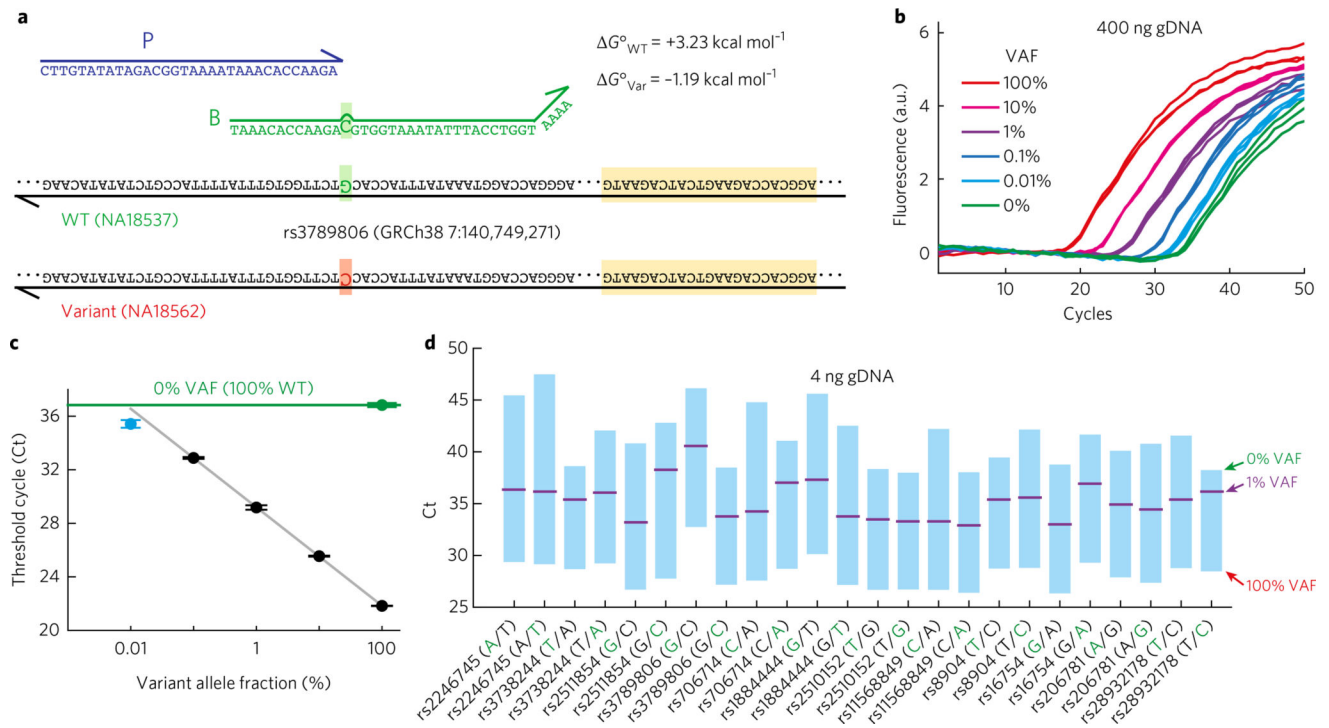
Fig. 2. Quantitative PCR results on BDA enrichment

a, Primer and blocker sequences for enrichment of the non-pathogenic rs3789806 SNP. The reverse primer sequence is highlighted in yellow. The NA18537 genomic DNA (gDNA) sample bears the homozygous WT allele, and the NA18562 gDNA sample bears a homozygous SNP variant. The 4 A sequence at the 3′ end of the blocker serves as a termination sequence to prevent the blocker from being elongated by the Taq polymerase during PCR. **b**, Triplicate qPCR results for various mixtures of NA18562 and NA18537 with different variant allele fractions (VAFs). Each sample consisted of 400 ng gDNA in total (corresponding to 120,000 haploid copies), with the indicated VAF fraction as NA18562 and the remainder as NA18537 (for example, 1% VAF = 4 ng NA18562 and 396 ng NA18537). Experiments were performed using the Applied Biosystems PowerUP supermix using a 2-step protocol alternating 10 s at 95 °C and 30 s at 60 °C. **c**, A summary of threshold cycle (Ct) values for the results observed in **b**. Error bars show 1 standard deviation; 0.01% VAF data points are not included in linear fit. **d**, A summary of qPCR results for 24 different BDA designs to 12 non-pathogenic SNPs; both allelic variants of each SNP were enriched using BDA in separate experiments. The green nucleotide indicates the allele to which the blocker is designed to suppress amplification. The bottom edge of the blue bars indicate the median Ct of the 100% VAF sample, the upper edge of the blue bars indicates the median Ct of the 0% VAF sample, and the purple line indicates the median Ct of the 1% VAF sample. Here, 4 ng gDNA samples were used for each experiment. See Supplementary Section 3 for raw qPCR traces.
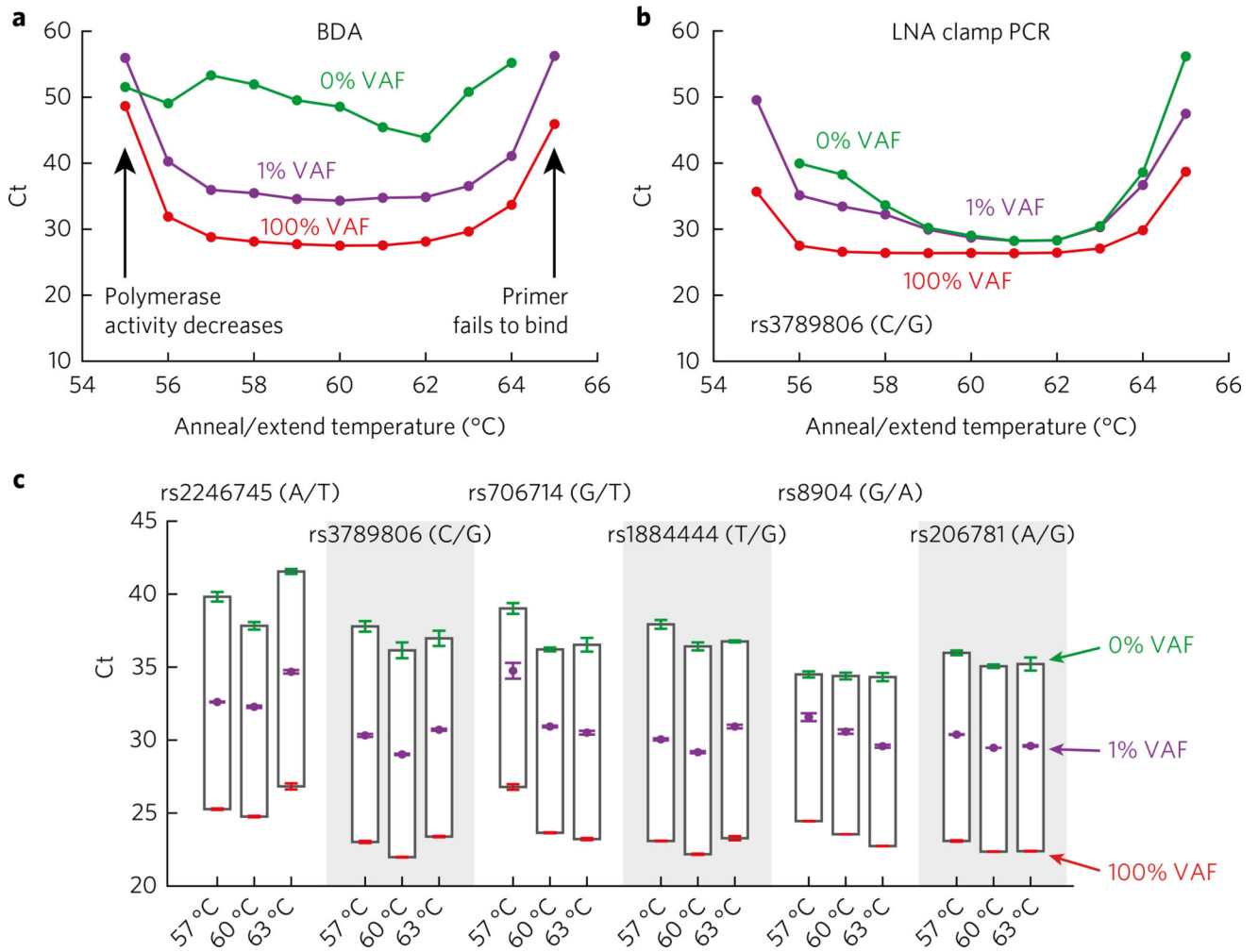
Fig. 3. Temperature robustness of BDA

a, Summary of Ct values for different anneal/extend temperatures; 4 ng gDNA input; see Supplementary Section 3 for raw qPCR traces. The BDA system efficiently enriches variants across an 8 °C temperature range, from 56 to 64 °C. **b**, Comparative performance of PCR allele enrichment through use of an LNA clamp. Because the binding of the LNA clamp is temperature sensitive, a significant Ct is observed only between 56 and 57 °C. Even at the optimized temperature of 57 °C, Ct values for LNA clamp PCR are lower than for BDA. **c**, Temperature robustness validation for five additional SNPs. All tested BDA designs maintain Ct 10 at temperatures from 57 to 63 °C; 200 ng gDNA input.

Fig. 4.
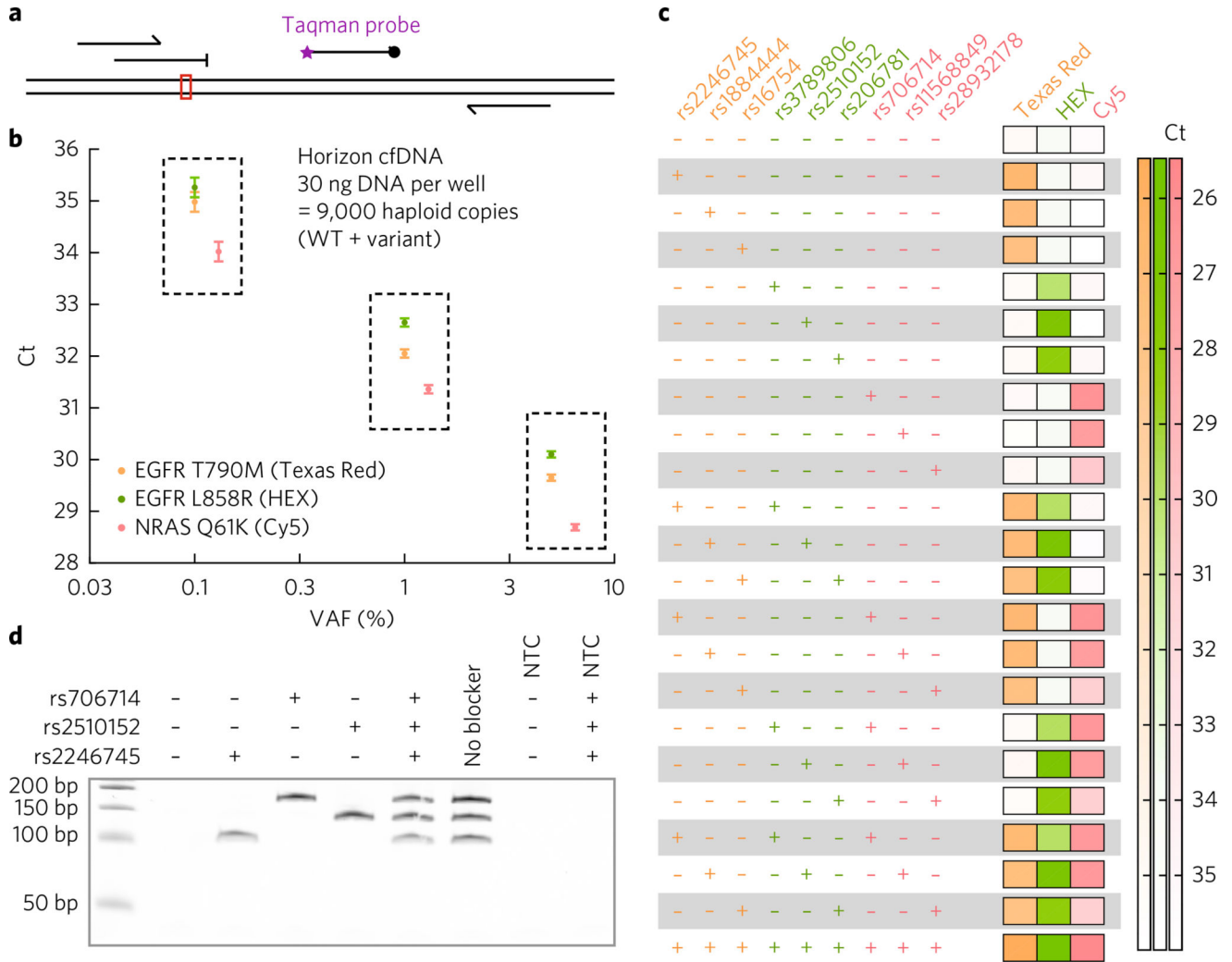
a, Non-allele-specific Taqman probes are used for multiplex BDA readout. **b**, Three-plex BDA on Horizon Discovery cell-free DNA reference samples. Each dashed box represents a different reference sample with varying VAF values of the three cancer mutations of interest. The final concentration of forward and reverse primers are 100 nM each, blockers are 1 μM each, and Taqman probes are 100 nM each. The samples used were purchased from Horizon Discovery (catalogue number HD780). Each cancer mutation is reported by a different Taqman probe as shown in the legend; reported Ct values and ranges are mean and standard deviations for 3 independent experiments each. **c**, Nine-plex BDA to non-pathogenic SNPs. Each reaction (horizontal row) employs different combinations of blockers to different alleles, but uses the same NA18537 sample. Minus signs indicate where the corresponding blocker suppresses the NA18537 allele, and plus signs indicate where the blocker suppresses an alternative allele. Thus, '+ ' reactions are designed to provide significant amplification (low Ct). The final concentration of forward and reverse primers are 50 nM each, and the concentration of the blockers are 500 nM each; 4 ng NA18537 input. See Supplementary Section 7 for details and qPCR traces. **d**, Multiplexed BDA using the portable and inexpensive MiniPCR instrument. Three different BDA systems were designed

simultaneously to amplify select alleles of the rs706714, rs2510152 and rs2246745 SNPs; amplicons lengths were 171, 138 and 107 nt, respectively, which are clearly distinguished on the 10% denaturing polyacrylamide gel. See Supplementary Section 8 for details.
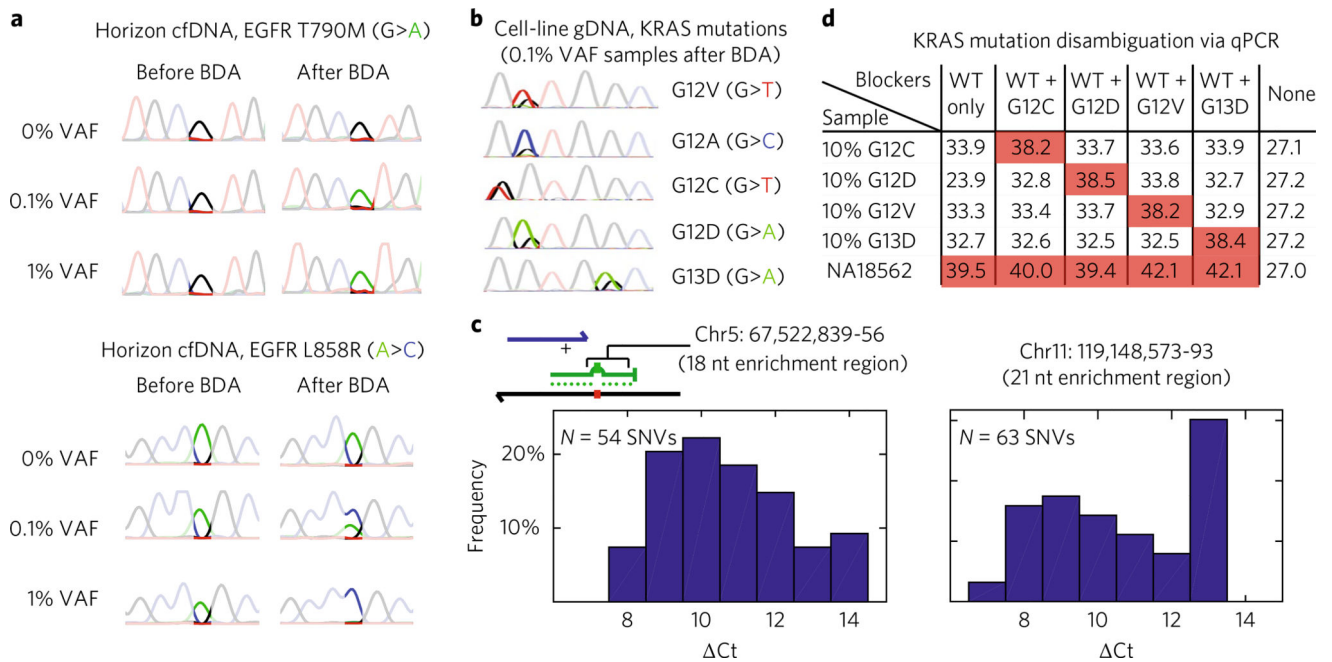
a, Sanger sequencing verification that BDA enriches rare mutants. Experimental results on Horizon cell-free DNA (cfDNA) reference samples before and after BDA. Before BDA, the cancer mutation is not visible even at the 1% VAF level; after BDA, the cancer mutation is the dominant peak for both the 0.1% and 1% VAF samples. The 0% VAF samples still show the WT allele as the dominant peak after BDA enrichment, indicating that BDA has not spuriously introduced nonexistent variants. **b**, A single-plex BDA enriches 0.1% VAF of 5 KRAS mutants from cell-line gDNA; Sanger sequencing results of amplicon products confirm the enrichment of the appropriate mutant alleles. **c**, BDA preferentially amplifies all variants within the enrichment region. The left panel shows the distribution of experimental Ct values observed for the same BDA primer/blocker set to 54 synthetic templates each bearing a SNV within an 18 nt enrichment region, and the right panel shows the Ct value distribution for 63 synthetic SNV templates for a different BDA system. Indicated genomic coordinates are based on GRCh37.p13. See Supplementary Section 9 for qPCR traces; Ct values are the median of triplicates. **d**, Variant disambiguation in qPCR setting using a blocker specific to the variant of interest. The simultaneous use of a WT blocker and a mutant blocker produces weak amplification (high Ct, red shading) when no incidental SNPs are present, but strong amplification (low Ct) if one or more incidental SNPs are present. Ct values shown are the median of triplicates.
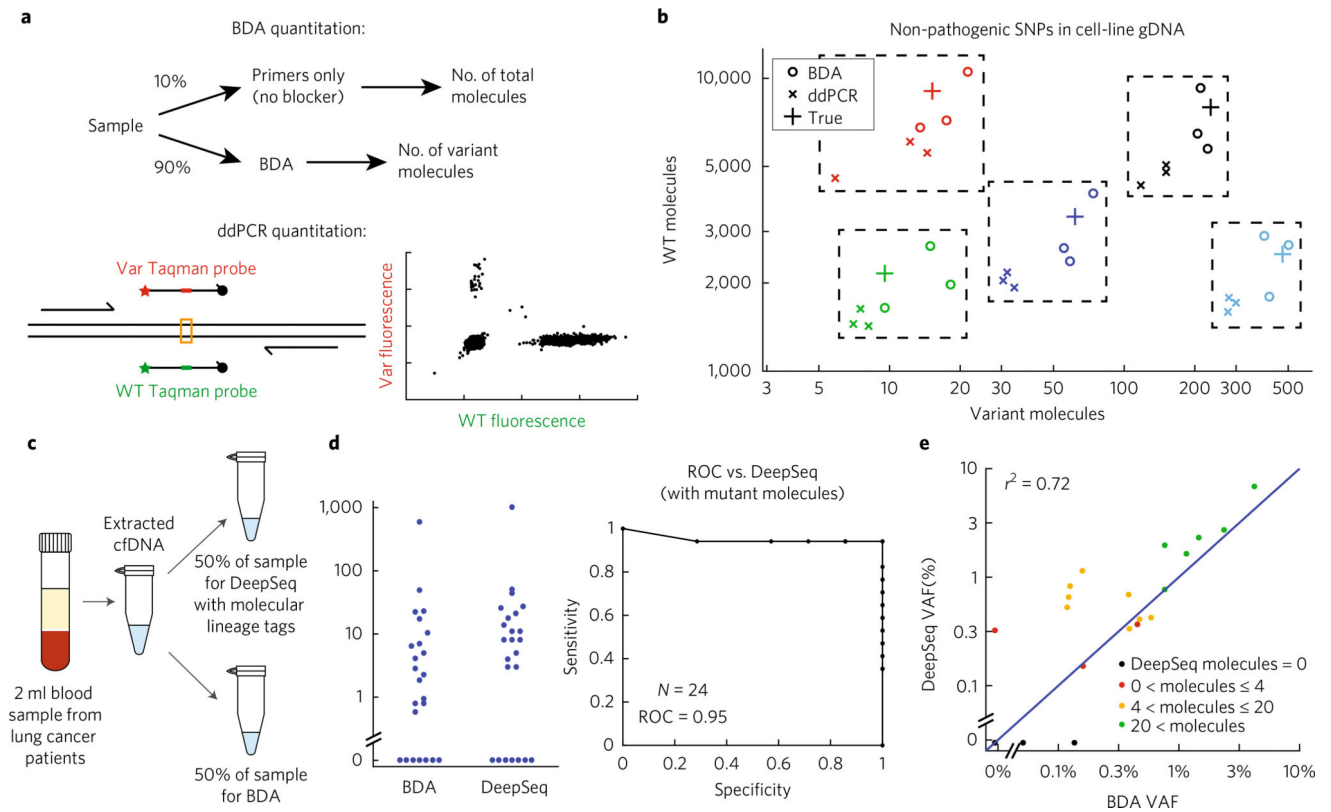

Fig. 6. Rare allele quantitation with BDA

a, To quantitate the VAF of a variant within a sample, we asymmetrically split the sample and ran two separate qPCR reactions: 10% of the sample is amplified using the primers but without blocker, in order to quantatite the total number of molecules of the relevant gene locus; 90% of the sample is amplified using BDA to determine the number of variant molecules. Note that this quantitation process can be multiplexed using different Taqman probes as shown in Fig. 4. For comparison, we also quantitated VAF using Biorad droplet digital PCR (ddPCR). ddPCR quantitation employs two separate Taqman probes, one to the variant and the other to the WT, and cannot be multiplexed. **b**, Experimental results on quantitating non-pathogenic SNP VAFs. Five different reference genomic DNA samples were constructed by mixing NA18537 (variant) and NA18562 (WT). True values, BDA quantitated values, and ddPCR quantitative values for the same reference samples are grouped together in boxes. Based on these results, BDA and ddPCR quantitation accuracies appear comparable; see Supplementary Section 11 for quantitation results on Horizon cfDNA reference samples. **c**, Quantitating rare mutations in 24 clinical cell-free DNA samples from lung cancer patients. Samples were split, with half being used for BDA quantitation and the other half being used for deep sequencing quantitation using molecular lineage tags as described previously[35,47]. Seven different mutations in the KRAS, EGFR, NRAS and PIK3CA genes were tested (see Supplementary Section 12). **d**, The inferred numbers of mutant molecules using BDA and deep sequencing, and receiver operator characteristic (ROC) accuracy of BDA versus deep sequencing in the determination of mutationpositive samples. There is only one discordant sample, in which BDA did not detect any mutant molecules, but deep sequencing detected three; this is likely to be due to sample

splitting with a small discrete number of total mutant molecules. **e**, Comparison of inferred VAF using BDA versus deep sequencing.

Table 1

A comparison of rare mutation detection technologies

Method	Mutation LoD (%)	No. of potential mutations	Protocol time (h)	Cost per sample (US$)	Instrument cost (US$)
BDA	**0.1**	**100–1,000**	**2**	**3**	**650**
ARMS	1–10	< 4	**2**	**3**	10,000+
ARMS (castPCR)	**0.1**	4	**2**	**3**	10,000+
NGS	1	**1,000+**	48+	1,000+	100,000+
NGS(SafeSeq/CAPPseq)	**0.1**	**1,000+**	48+	1,000+	100,000+
Microarray	1–10	**1,000+**	16+	1,000+	100,000+
Microarray (MIP)	**0.1–1**	**1,000+**	48+	1,000+	100,000+
Digital PCR	**0.1**	1	**4**	**10**	100,000+

Innovations to the basic ARMS[13], NGS[16],and microarray[45,46] technologies have improved mutation sensitivity, but BDA is unique in simultaneously providing good mutation sensitivity (low limit of detection, LoD), high mutation multiplexing, fast turnaround, and low reagent and instrument cost. Bold or not bold indicate that a technology objectively performs well (bold) or not so well (not bold) on the given metric.